Available online at www.sciencedirect.com

SciVerse ScienceDirect

Journal of the European Ceramic Society 32 (2012) 1067–1075

www.elsevier.com/locate/jeurceramsoc

Innovative fabrication of PZT pillar arrays by a colloidal approach

Susana M. Olhero [a,b,*], Luis Garcia-Gancedo [b], Tim W. Button [b], Fernando J. Alves [a], José M.F. Ferreira [c]

[a] Department of Mechanical Engineering and Industrial Management, FEUP, University of Porto, Porto, Portugal
[b] IRC in Materials Processing, School of Metallurgy and Materials, University of Birmingham, Birmingham, B15 2TT, UK
[c] Department of Ceramics and Glass Engineering, CICECO, University of Aveiro, Aveiro, 3810-193, Portugal

Received 5 July 2011; received in revised form 2 November 2011; accepted 12 November 2011
Available online 16 December 2011

Abstract

An innovative approach for fabricating pillar arrays for ultrasonic transducer applications is disclosed. It involves the preparation of concentrated piezoelectric lead zirconate titanate (PZT) suspensions in aqueous solutions of epoxy resin and its polymerization upon adding a polyamine based hardener. Zeta potential and rheological measurements revealed that 1 wt.% dispersant, 20 wt.% of epoxy resin and a hardener/epoxy resin ratio of 0.275 mL g^{-1}, were the optimized contents to obtain strong PZT samples with high green strength (35.21 ± 0.39 MPa). Excellent ellipsoidal and semi-circle shaped pillar arrays presenting lateral dimensions lower than 10 μm and 100 μm height were successfully achieved. The organics burning off was conducted at 500 °C for 2 h at a heating rate of 1 °C min^{-1}. Sintering was then carried out in the same heating cycle at 1200 °C for 1 h. The microstructures of the green and sintered ceramics were homogeneous and no large defects could be detected.

Keywords: A. Suspensions; A. Shaping; D. PZT; E. Sensors; Gel casting

1. Introduction

1–3 piezocomposites with pillars of piezoelectric ceramic surrounded by an epoxy matrix are the standard active materials in ultrasonic transducers operating at conventional frequencies (<20 MHz). Higher frequency transducers are needed to improve resolution in areas such as dermatology and ophthalmology, but their development is limited by the difficulty of fabricating fine scale pillar arrays. Current fabrication techniques are incompatible with both the dimensions and designs necessary for such frequencies, and although new instrumentation is emerging for ultrahigh resolution biomedical imaging, practical devices are still unavailable at such frequencies.[1]

Hence, one of the biggest challenges in developing sensitive transducers and arrays for real-time high frequency (>30 MHz) biomedical ultrasound imaging lies in the fabrication of fine scale pillar arrays for piezocomposites. Piezocomposites are now made almost exclusively by the dice-and-fill technique, whereby deep grooves are cut into a solid sintered ceramic block with a thin dicing blade to create a bristle-block comprising thin, tall square pillars upstanding from a support stock. Then a polymer is cast into these grooves, and the resulting composite disk sliced off the ceramic base.[2] While this technique is sufficient enough to make the standard medical imaging transducers operating up to 20 MHz,[2] the fabrication of composites for higher frequencies becomes very difficult because of the ultrafine lateral features required for efficient operation. Therefore, other fabrication methods to make transducers that can operate at higher frequencies must be sought. Some well-known general purpose alternatives to dice-and-fill are injection moulding,[3] laser micromachining,[4] interdigital pair bonding[5] or viscous polymer processing (VPP).[6]

Gel casting (GC) is one of the best performing techniques developed so far to fabricate complex-shaped ceramic bodies from low viscosity slurries that can be solidified by gelation once the mould is filled, thus facilitating mould removal prior drying and sintering.[7–11] A number of gelation systems, such as, polysaccharides,[12,13] monomers and crosslinkers,[9–11,14–17] have been already proposed. In the most common process, the ceramic powders are dispersed in a pre-mixed solution of monomers,

* Corresponding author at: Department of Mechanical Engineering and Industrial Management, FEUP, University of Porto, Porto, Portugal.
Tel.: +351 234 370261; fax: +351 234 370204.
E-mail address: susana.olhero@ua.pt (S.M. Olhero).

0955-2219/$ – see front matter © 2011 Elsevier Ltd. All rights reserved.
doi:10.1016/j.jeurceramsoc.2011.11.016

dimmers and a cross linker to obtain a high solids loading slurry. An initiator is then added and homogenised and the suspension cast in a mould of the desired shape. The monomer and cross linker polymerize and form a three-dimensional network structure, thus transforming the slurry into an *in situ* solidified green body under controlled atmosphere. Although GC has been successful in producing both large to small size components, it is not suitable for the fabrication of micro-sized components because the green strength is insufficient to withstand the high shear stresses generated upon demoulding.[10,15,16]

Recently, a self-hardening gel-casting method based on a thermosetting resin and hardener was reported by Mao et al.,[18,19] which could be carried out in an air atmosphere. The main requirement for this processing is finding suitable water soluble epoxy resin and hardener that must be compatible with the powder and dispersant. Different epoxy resins have been already used for consolidating alumina ceramics with large dimensions.[18–20] However, the green strength achieved was also too low to enable fabrication of micro components. Hence, developing a new colloidal approach to produce strong piezoelectric micro components would have high scientific, technological, and economic impacts.

Inspired by previous studies, the aim of this work is to develop a new consolidation process based on the curing of a high solids loading slurry to obtain ultra-fine piezoelectric pillar arrays. For that, high concentrated suspensions were prepared by dispersing lead zirconate titanate (PZT) powders in an aqueous solution of an epoxy resin, dispersant and hardener. The results of the characterization of the suspensions and of the consolidated green and sintered samples are presented and discussed systematically.

2. Experimental procedure

2.1. Materials and reagents

A PZT powder (TRS 610C, TRS Technologies, USA) with 7.94 g cm^{-3} density, milled to an average particle size d_{50} = 0.49 μm (Coulter LS 230, Buckinghamshire, UK, Fraunhofer optical model) and BET specific surface area of 1.76 m^2 g^{-1} was used. Dispex A-40 (Allied Colloids, Bradford, UK), an ammonium polyacrylate ($NH_4$$^+$PAA, molecular weight of 3500 g mol^{-1}) solution was selected as dispersant. An epoxy resin, ethylene glycol diglycidyl ether (EGDE, Sigma–Aldrich, Germany, 1.152 g cm^{-3}) soluble in aqueous media and, a polyamine hardener, bis(3-aminopropyl) amine (Sigma–Aldrich, Germany, 0.958 g cm^{-3}) were employed as consolidating agents.

2.2. Suspensions preparation and characterization

Preliminary tests were performed by dispersing 35 vol.% of PZT powder into an aqueous solution containing 17.5 wt.% of epoxy resin and different added amounts of Dispex in order to select the most appropriate amount of dispersant (1 wt.% based on dry solid matter). Then, the concentration of epoxy resin in the dispersing solution was varied (10; 12.5; 17.5; and 20 wt.%) and flexural strength testing PZT bar shaped samples with 50 × 10 × 5 mm were consolidated aiming at green strength maximization. Zeta-potential of PZT powder was measured (Malvern Zeta sizer, Nano ZS, Malvern, Worcestershire, UK) in the absence and in the presence of dispersant and epoxy resin using 1 mM KCl solution as background electrolyte. pH adjustments were performed by adding 0.1 M solutions of either NH_3 or HNO_3. The viscosity of suspensions was measured using a rotational rheometer (Bohlin Instruments, C-VOR, Worcestershire, UK) within the shear rate range of 0.1–500 s^{-1} with a cone and plate (4, 40 mm, gap 150 μm) measuring configuration. PZT samples in the absence and in the presence of resin with or without dispersant were analyzed by Fourier Transform Infrared spectroscopy (FT-IR, model Mattson Galaxy S-7000, USA) and compared to the spectrum of the resin alone in order to assess how the epoxy resin is linked to the surface of PZT powder particles.

2.3. Fabrication of pillar arrays

Elastomeric soft moulds were fabricated by replication from master templates using PDMS – Sylgard Silicone Elastomer 184 and Sylgard Curing Agent 184 (Dow Corning Corporation Limited, Coventry, UK). Master templates of the appropriate structure were placed in a glass Petri dish; then a 10:1 weight ratio mixture of PDMS and curing agent was poured onto the master template in a vacuum desiccator and de-aired. The de-airing step is particularly important due to the small kerfs between the pillars. The PDMS was cured at 67 °C for 4 h. After cooling to room temperature, the soft PDMS was peeled from the master template and checked for defects under the microscope. The ceramic suspension was then cast into the mould in a vacuum desiccator system for 1–2 min to aid full penetration of the suspension into the moulded structures and assist further de-airing. After 24 h consolidation at room temperature, the mould was carefully peeled off to leave the patterned green pillar arrays on a ceramic base or stock. The green bodies were then completely dried in an air oven at 100 °C. The dried rectangular bars were used for linear shrinkage, the 3-point bend strength using an Instron testing machine (Instron, Buckinghamshire, UK), and density measurements according to the Archimedes principle. Thermal analysis (TG/DTA – Setaram, Labsys, Caluire, France) was used to study burning off the resin and hardener through weight loss and heat flow of the dried PZT samples in air atmosphere at a heating rate of 10 °C min^{-1} until 600 °C. Based on these results, the organics burning off was conducted at 500 °C for 2 h at a heating rate of 1 °C min^{-1}. Sintering was carried out at 1200 °C for 1 h. Photographs of pillar arrays with different shapes were taken in a Jeol 7000F SEM. The fracture surfaces of green and sintered PZT samples were observed by scanning electron microscopy (Hitachi S-4100, Tokyo, Japan).

3. Results and discussion

Fig. 1 shows the particle size distributions of PZT powders as received and after 12 h of vibro milling in ethanol. It can be seen that the as received PZT powder presents a bimodal distribution, with a particle populations centred at ≈0.3 μm and

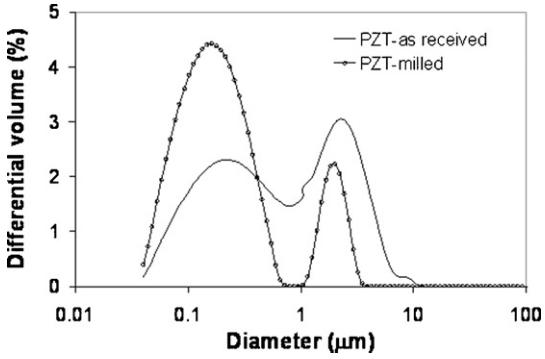

Fig. 1. Particle size distributions of PZT powders as received and after 12 h vibro milling.

≈3 μm respectively. After milling, the volume fraction of the first population increased with a concomitant decrease of the coarser one, resulting in an overall decrease of average size, d_{50}, from 1.3 to ~0.5 μm. The presence of two particle populations with different sizes is expected to increase the particle packing ability in a slurry, since the smaller particles could occupy the interstitial spaces between the larger ones and release the liquid immobilised in void spaces.[21] In this way, bimodal particle size distributions enable a decrease in viscosity for a given solids loading, or the use of a higher solids volume fraction while maintaining a given viscosity level, a key point for successfully fabricating ceramics by direct consolidation techniques. It is known that for a given dispersant there is an optimum concentration that minimises the viscosity of the suspension. Lower amounts are insufficient to cover all the available surface area of the particles and to shield the attractive Van der Waals forces. On the other hand, if too much dispersant is added, the excess will remain in solution increasing the ionic strength and the viscosity of the dispersing media.[22] Therefore, evaluating the influence of dispersant concentration on viscosity is of a paramount importance.

Fig. 2 shows the effect of dispersant on the viscosity of PZT suspensions containing 35 vol.% solids loading, measured at a steady shear rate of 125 s^{-1}, in the absence and in the presence of 17.5 wt.% of resin. Viscosity decreases with increasing added

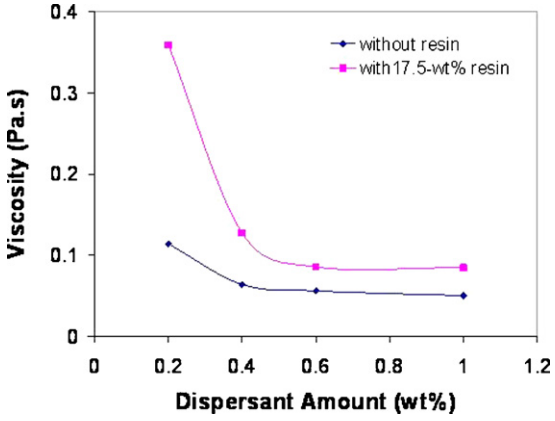

Fig. 2. Viscosity measured at the steady shear rate of 125 s^{-1} of suspensions with 35 vol.% of milled PZT powder as a function of the added amount of dispersant, in presence and in the absence of 17.5 wt.% epoxy resin.

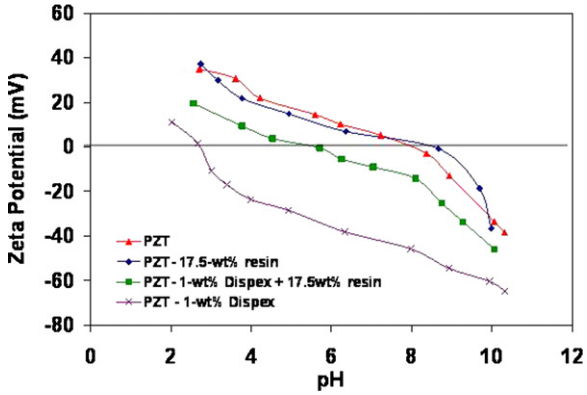

Fig. 3. Zeta potential curves of PZT particles as a function of pH measured in the absence of processing additives and in the presence of dispersant or resin or both.

amounts of dispersant achieving a minimum plateaux within the range of about 0.6–1.0 wt.% dispersant. Furthermore, viscosity values are systematically higher in the presence of epoxy, meaning that the relative viscosity of dispersing medium (the ratio of the viscosity of the resin solution to the viscosity of distilled water) has increased, therefore enhancing the resistance of the suspension to flow. But the differences in viscosity levels along the minimum plateaux are smaller than would be expected from the enhanced viscosity of the resin solution, suggesting that the resin has some synergetic effect on dispersing the PZT powder. Moreover, the variation of viscosity with increasing amounts of dispersant is much sharper in the presence of epoxy resin. This observation suggests that the adsorption of polyanions of Dispex A-40 at the surface of PZT particles is enhanced in the presence of resin molecules. This could be understood if resin species of cationic nature have been adsorbed at the surface of PZT particles. In order to shed light on the specific interactions of the different dissolved species on the solid/liquid interface, zeta potential measurements were performed as a function of pH in the absence of processing additives and in the presence of dispersant or resin or both.

Fig. 3 shows that the isoelectric point (IEP) for the PZT powder is located at about pH 8. This means that in absence of processing additives, a neutral or slightly alkaline environment is not suitable for a good dispersion necessary for the preparation of high solids loading suspensions. The presence of 17.5 wt.% of resin had a negligible effect on zeta potential but the IEP was shifted to about pH 8.4, suggesting that resin molecules have been adsorbed at the surface of the PZT particles and possess a slightly cationic nature. This would favour a more extensive adsorption of the anionic dispersant, as hypothesised above, and contribute to the observed sharper decrease of viscosity with increasing added amounts of dispersant (Fig. 2). Conversely, the presence of 1 wt.% of Dispex A-40 alone caused a shift of the IEP to around pH 2.6 and negative zeta potential values as high as −60 mV at the natural pH of the suspensions (≈pH 10–10.3). This confirms the accentuated anionic nature of the dispersant and its suitability to prepare stable and concentrated aqueous suspensions. In the presence of Dispex A-40 + 17.5 wt.% resin, the isoelectric point is located at around pH 5.5, i.e., exactly at

the intermediate position between the IEPs measured in the presence of each processing additive alone, 2.6 and 8.4, respectively. The results shown in Fig. 3 reveal that electrostatic interactions became weaker in the presence of resin, which also increases the viscosity of the dispersion medium. Even though, the viscosity levels along the minimum plateaux of the systems with and without resin do not differ so much, suggesting that the resin may be contributing to dispersion through other kind of interactions.

Colloidal stability is governed by the total interparticle potential energy, V_{total}, which can be expressed as:

$$V_{total} = V_{vdW} + V_{elect} + V_{steric} + V_{structural} \quad (1)$$

where V_{vdW}, is the attractive potential energy due to long-range van der Waals interactions between particles, V_{elect}, is the repulsive potential energy resulting from electrostatic interactions between like-charged particle surfaces, V_{steric}, is the repulsive potential energy resulting from steric interactions between particle surfaces coated with adsorbed polymeric species, and $V_{structural}$ is the potential energy resulting from the presence of non adsorbed species in solution that may either increase or decrease suspension stability. The attractive van der Waals forces depend on the nature of the particles and of the solvent, while repulsive electrostatic forces are directly dependent on the zeta potential developed at the solid/liquid interface and can be modified by the presence of processing additives in solution,[22,23] as observed in Fig. 3.

According to Derjaguin–Landau–Verwey–Overbeek (DLVO) theory,[24–26] a high zeta potential of around 40 mV is necessary to electrostatically stabilize aqueous high solids loaded suspensions required for near-net shaping of ceramics.[23] The establishment of repulsive interaction forces strong enough to overcome the van der Waals attractive ones that tend to hold particles together is necessary. Fig. 3 shows that at the natural pH of the suspensions (≈pH 10–10.3) the absolute values of zeta potential are enough high (∼40 mV) to promote electrostatic stabilization. Moreover, the other contributions to stabilization predicted in Eq. (1) cannot be excluded.

In an attempt to get evidences about the specific interactions of resin molecules with the surface of PZT particles, FT-IR analysis of the resin and of PZT alone, and of different combinations of PZT and the processing additives as follows: (i) PZT + resin; (ii) PZT + dispersant; (iii) PZT + resin + dispersant before resin cure; (iv) PZT + resin + dispersant after resin cure, were carried out. The results are presented in Fig. 4. The characteristic bands of PZT perovskite structure could be witnessed at around the following wave numbers:[27–29] (i) 575 cm^{-1}, accounting for the stretching vibrational mode of Ti–O and Zr–O bonds; (ii) 1150 and 1395 cm^{-1} attributed to lead titanate. The spectrum of resin presents characteristic bands at 851.6, 904.6, 1085, 1245, 1612 and 2868 cm^{-1}, corresponding to the vibration of the several chemical bonds in the structure as assigned in Table 1.[29,30] The resin picks corresponding to the aromatic connections, namely at 851.6, 904.6, and 1245 cm^{-1}, for C–H_2, C–H and C–O, respectively, disappeared after cure, while the intensities of the picks at 1085 and 1385 cm^{-1} decreased. These observations suggest

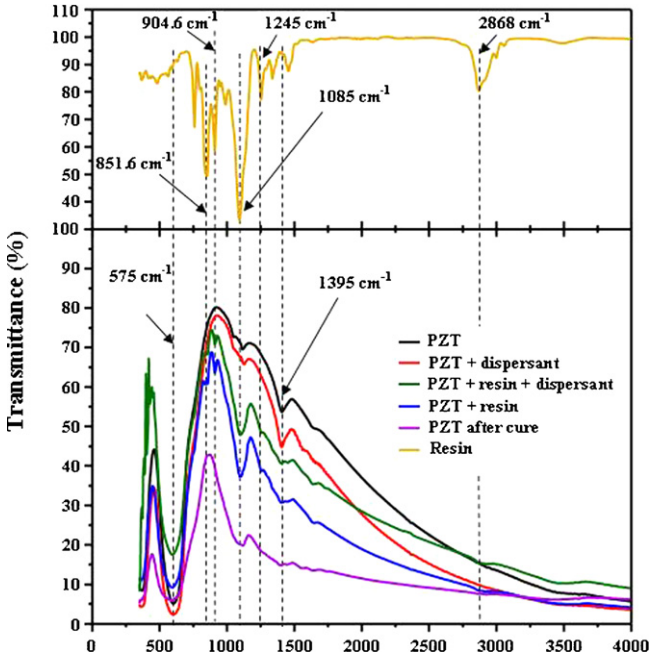

Fig. 4. FT-IR analysis of resin molecules and PZT in presence and in absence of resin and dispersant.

that some changes in the resin molecule occurred in presence of the hardener originating a different structure.

But the main aim of FT-IR analysis was to shed some light on the specific interactions between the resin molecules and the surface of PZT particles. The transmittance bands show that the presence of dispersant does not affect the PZT spectrum, meaning that it is adsorbed at the surface of PZT particles through small intermolecular forces. However, the intensities of the adsorption picks corresponding to the resin in the system PZT + resin + dispersant, namely at 851.6, 904.6, 1085 cm^{-1}, are lower when compared with those observed in the PZT + resin. The differences observed emphasise the competitive adsorption of both processing additives at the surface of PZT particles, in close agreement with the zeta potential data reported in Fig. 3. These specific interactions can be understood based on the molecular structure of the resin and its dependence on the chemical environment, as discussed below.

Fig. 5 shows a schematic representation of the molecular structure of the resin in the solution (Fig. 5a), and adsorbed at the surface of PZT particles in the absence (Fig. 5b), and in the

Table 1
Wave number picks of PZT and resin and the corresponding group vibrations.[29,30]

Wave number (cm^{-1})	Compound	Vibrations assignment
575	PZT	Ti–O and Zr–O
851.6	Resin	C–H_2 aromatic
904.6	Resin	C–H aromatic
1085	Resin	C–O aliphatic ether
1105	PZT	Lead titanate[29]
1245	Resin	C–O aromatic ether
1395	PZT	Lead titanate[29]
2868	Resin	C–H aliphatic symmetric

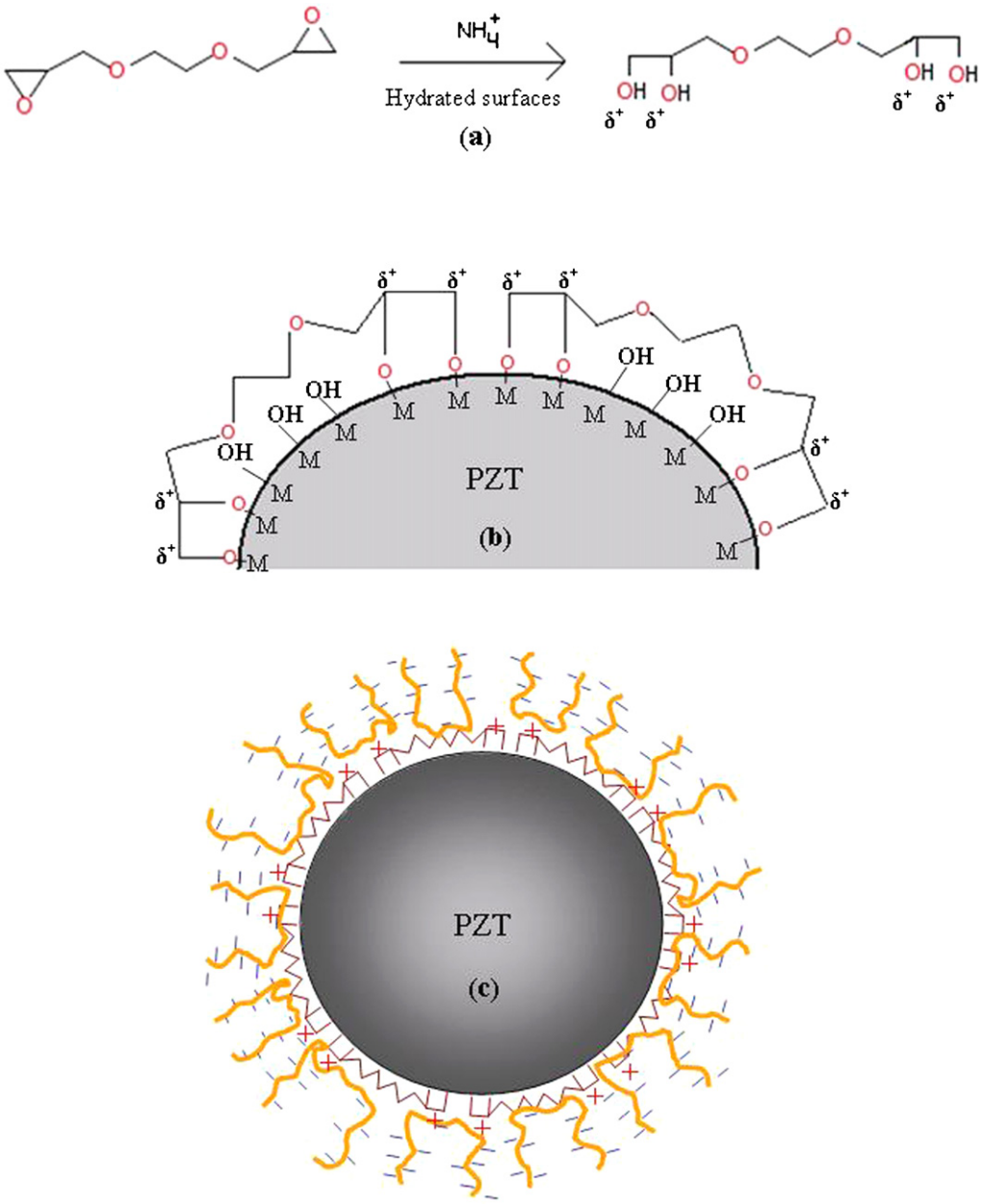

Fig. 5. Schematic representation of the: (a) molecular structure of the ethylene glycol diglycidyl ether, the unlocking of the epoxy groups at the edges under alkaline environment and in the presence of hydrated surfaces creating dipoles in the vicinity; (b) adsorption of the epoxy resin onto the surface of the PZT particles; (c) electrosteric stabilization of PZT particles in presence of resin and dispersant.

presence of dispersant (Fig. 5c). The epoxy groups at the edges of the molecule become very unstable due to the high stresses within the ring connections. Under alkaline conditions and in the presence of hydrated surfaces/ammonium groups (NH_4^+PAA) derived from the dispersant or amines, these rings are susceptible to unlock and give rise to the formation of two hydroxide groups, consequently distorting the electrical charge and creating dipoles in the vicinity as suggested in the right hand side of Fig. 5a. These polarized species are prone to readily absorb onto hydrated surfaces through the OH groups as suggested in Fig. 5b. This would explain the slight cationic character of the resin by shifting the IEP towards the alkaline pH region (Fig. 3). The positive dipoles at the outer surface of the adsorbed resin molecules will act as an additional driving force for the adsorption of anionic species from the dispersant. Therefore, a more extensive adsorption of the dispersant is expected in the presence of resin molecules. At the natural pH of the suspensions, the functional groups along the polyelectrolyte chains of the dispersant will be fully dissociated as suggested in Fig. 5c. However, the partial neutralization effect exerted by the positive dipoles of the resin molecules results in a decrease of electrostatic repulsive forces as deduced from the zeta potential measurements. But this does not necessarily mean an overall decrease of repulsive forces among the particles since the fully dissociated polyelectrolyte chains repelling each other and extending to the solution are likely to exert a steric hindrance. Due to the overall charge

neutralization effect exerted by resin molecules, the stretching of the dissociated polyelectrolyte chains to the solution will be enhanced when resin is absent. This is to say that the apparent radius (hard radius + add layer thickness) of the PZT particles dispersed is expected to be higher in the absence than in the presence of resin. This means that the interaction distance, i.e., the distance at which particles start to feel the presence of their neighbours might be larger in the absence of resin. In other words, the effective volume fraction of solids, ϕ_{eff}, can be given by the relation below, where δ is the ad layer thickness, a is the particle radius, and ϕ is the solids volume fraction:

$$\phi_{eff} = \phi\left(1 + \frac{\delta}{a}\right)^3 \quad (2)$$

Under these circumstances, the increase of the relative viscosity of the resin solution can be mitigated by a decrease of the ad layer thickness and a synergetic steric contribution for dispersing the PZT particles. The range of steric interactions is shorter in comparison to electrostatic ones, contributing to the decrease in the viscosity of the suspensions. This is beneficial for increasing solids loading, the homogeneity of the slurries, and for casting them into moulds with small features such as ultra-fine piezoelectric ultrasonic pillar arrays.

According to Mao et al.[19] the polymerization between the epoxy group of the resin and the active hydrogen of the amine is a nucleophilic addition reaction rather than a free radical reaction, and is therefore not inhibited by oxygen from the air atmosphere. Hence, the processing of the microstructures can be carried out under environmental temperature and humidity conditions. The polymerization of the suspensions with different added amounts of epoxy resin and respective hardener was monitored by registering the changes of storage modulus (G′) and loss modulus (G″) at room temperature (RT) and at 40 °C, to study the effects of resin content and temperature on the gelation behaviour. At RT both the parameters G' and G'' increased with time increasing, with predominance of G'' up to the crossover point where the situation was reversed. The crossover of G′ and G″ curves is conventionally taken as the gelation point from which the elastic modulus, G′, increases faster than the loss modulus, G'', and the elastic character predominates for the remaining gelation process leading to formation of a rigid gel. The gelation time decreased from > 80 min to, 35, 19 and 17 min for added amounts of resin of 10, 12.5, 17.5 and 20 wt.%, respectively, while the gel strength increased with increasing amounts of added epoxy resin, giving a good prediction trend for the green strength of cast samples. For the suspension with 10 wt.% resin, the gelation time was shortened from >80 min at 20 °C to 2 min at 40 °C, being further accelerated with increasing added amounts of resin. For the two higher amounts of resin the crossover point could not be unambiguously detected at 40 °C since gelation occurred within the time period required to set up the experiment. Based on these results, room temperature was selected to consolidate the green bars and pillar arrays.

Table 2 shows the strong influence of resin content on the suspension properties and on the characteristics of green and sintered bodies consolidated by the new aqueous gel casting technique. Increasing the amount of resin has the following consequences: (i) the gelation time decreases; (ii) green density, percentage of linear shrinkage upon drying and green strength are all enhanced; (iii) sintered density tends to decrease. The effects of resin content on green properties can be understood by considering that the *in situ* gelation creates a 3D network of fine pores that exert a high suction pressure upon drying, making the gelcast samples to shrink. The fineness of the 3-dimensional porous network structure is exacerbated with increasing resin content. To prove this, homogeneous solutions containing 10 and 20 wt.% of epoxy resin + polyamine hardener in water were allowed to cure in cylindrical rubber moulds. Their measured apparent density and linear shrinkage are reported in Table 3. Considering that the theoretical density (TD) of the resin system is 1.11 g cm^{-3}, the percentages of TD (%TD) were 10.5% and 10.9% for 10 wt.% and 20 wt.% resin, respectively, meaning that these resin specimens consist of porosity fractions of 89.5% and 89.1%, respectively. The anchorage of resin molecules onto the surface of the particles, as sketched in Fig. 5b and c, and the enhanced fineness of the 3D network pores with increasing resin concentrations make the particles approach each other more upon drying under the stronger capillary forces generated. This explains the increase of drying shrinkage. The resin completely filling the interstitial pores among the PZT particles also accounts for the enhancement of the green density with increasing resin contents (Table 2).

The SEM micrographs of fracture surfaces of the PZT green samples consolidated from suspensions with different epoxy resin contents presented in Fig. 6 support this interpretation. At a first glance it seems that no remarkable differences exist among the samples. However, a more detailed analysis reveals that particles appear embedded in a kind of film that tends to fill the interstitial spaces among them, especially for the higher added amounts (17.5 and 20 wt.%) of resin. The noticeable roughness observed is not considered to be a result of porosity, but is typical of non-catastrophic failure due to pullout effects and to the resilience conferred on the samples by the cross linked polymer.

Enhanced particle packing together with the higher fractions of reinforcing cross linked polymer completely filling the interstices among the PZT particles are the responsible factors for the observed increase in green strength from about 15 to 35 MPa for epoxy resin contents increasing from 10 to 20 wt.%, respectively (Table 2). The flexural strength of 35 MPa is twice that measured for components consolidated by the traditional gelcasting process (18 MPa). Such high strength values allowed the ultra fine scale PZT pillar arrays with ellipsoidal and semicircle shapes having lateral dimensions lower than 10 μm and more than 100 μm height to be easily de-moulded as can be seen in the micrographs presented in Fig. 7. We have found that green bodies are resilient and can be significantly deflected before breaking, which is a key advantage for a successful de-moulding process. These results prove the suitability of the new aqueous gelcasting system for fabricating high green strength PZT micro components and microelectromechanical systems (MEMS).

However, the results of sintered density reported in Table 2 shown a clear decreasing trend with increasing amounts of added resin, suggesting that the relics of resin burning off have a

Table 2
Gelation time and properties of green and sintered PZT ceramics consolidated at room temperature by the new gelcasting process.

Sample	Gelation time (min)	Green density (g cm^{-3})	Linear shrinkage (%)	Green strength (MPa)	Sintered density (g cm^{-3})	Sintered TD (%)
PZT-10	>80	4.74 ± 0.09	2.84 ± 0.11	15.02 ± 0.79	7.89 ± 0.02	99.3 ± 0.3
PZT-12.5	35	4.94 ± 0.24	4.82 ± 0.16	25.13 ± 0.54	7.74 ± 0.01	96.7 ± 0.1
PZT-17.5	19	5.29 ± 0.23	5.86 ± 0.16	29.15 ± 0.25	7.42 ± 0.03	92.7 ± 0.4
PZT-20	17	5.28 ± 0.08	6.10 ± 0.09	35.21 ± 0.39	7.38 ± 0.02	92.2 ± 0.1

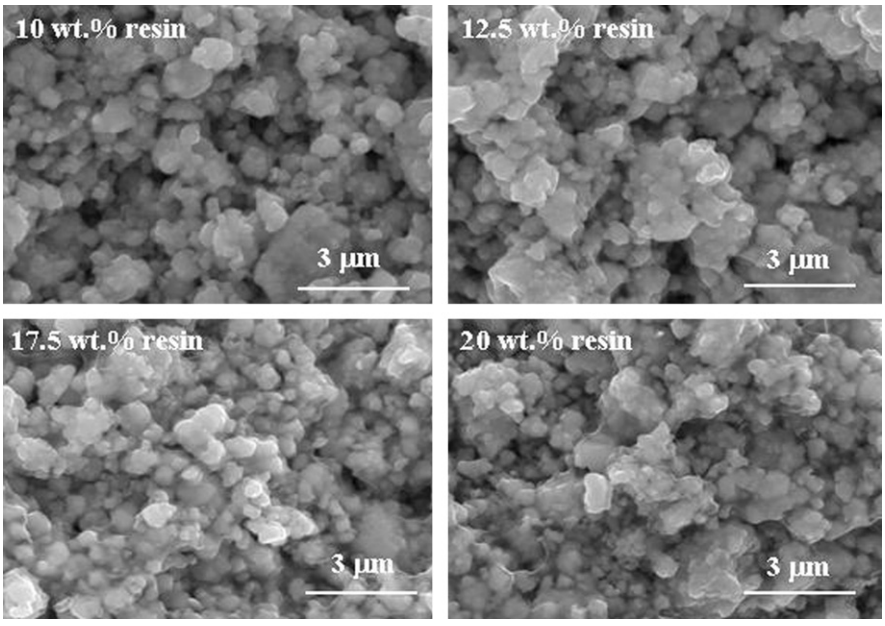

Fig. 6. SEM micrographs of PZT green samples obtained by the new gel casting technique with different added amounts of epoxy resin: (a) 10%; (b) 12.5%; (c) 17.5%; (d) and 20%.

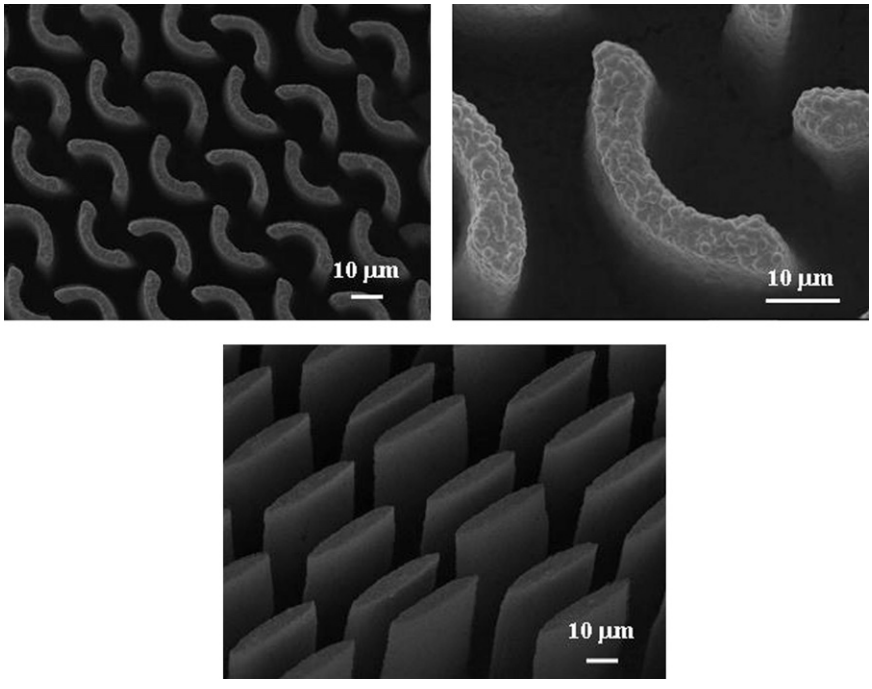

Fig. 7. SEM micrographs of green pillars arrays with different shapes: (a) view of half-circle pillars; (b) close-up of (a); (c) view of ellipse-shaped pillars.

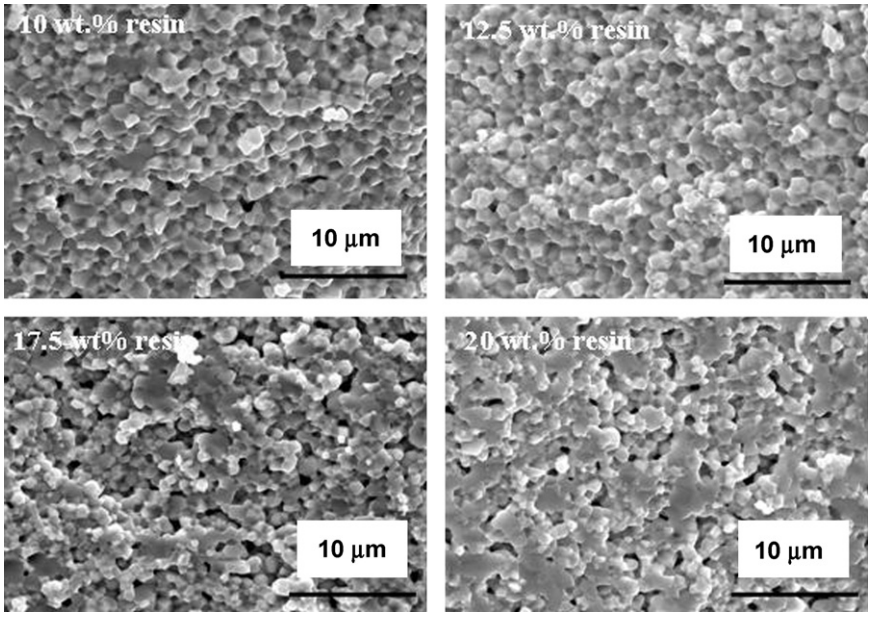

Fig. 8. SEM microstructures of PZT sintered samples obtained by the new gel casting technique with different added amounts of epoxy resin: (a) 10%; (b) 12.5%; (c) 17.5%; (d) and 20%.

deleterious effect on densification of PZT bodies. The burn off behaviour of the organic component was studied by thermal analysis in air atmosphere at the heating rates of 1 °C min^{-1} and 10 °C min^{-1} using very thin slices cut from the PZT sample containing 20 wt.% epoxy resin (results not shown). It was found that at the lower heating rate all the organics burnout up to about 400 °C, while the DTA signal was relatively weak. Increasing the heating rate to 10 °C min^{-1} caused an expected shift of the weight loss curve to higher temperatures and a constant weight was only achieved at about 500 °C. There was an initial slow weight loss step observed until ≈200 °C, corresponding to an endothermic effect, attributed to the release of free and adsorbed water. A second weight loss starting at ≈200 °C, corresponding to an overall exothermic effect, was due to the degradation of the organic additives, epoxy resin, hardener and dispersant, being in good agreement with the results obtained by other authors for similar organic compounds.[19,31] It is worthy to note that the total weight loss was between 9 and 10 wt.%, i.e., about double of that expected when considering only the added organic components (the percent of added resin is relative to the liquid media). This means that water is strongly retained in the cured resin. Based on these results, and considering the bulky features of the bars consolidated for flexural strength measurements, debinding experiments aimed at evaluating the influence of organic additives on the sintering process were conducted at 1 °C min^{-1} up to 500 °C, thus assuring a complete burnout of the organic substances before the sintering process starts.

Table 3
Apparent density and linear shrinkage of resin specimens consolidated at room temperature from solutions with different contents of resin.

Concentration of resin aqueous solution	Resin specimens	
	Apparent density (g cm^{-3})	Linear shrinkage (%)
10-wt.% resin	0.117 ± 0.004	39.10
20-wt.% resin	0.121 ± 0.006	23.20

Fig. 8 shows the SEM micrographs of fracture surfaces of sintered samples. A gradual increase of porosity with increasing amounts of resin is clearly noticed from these micrographs, in close agreement with the concomitant decrease in sintered densities (Table 2). These results support the hypothesis raised above that the burn off relics of resin have a deleterious effect on sintering ability, since the green packing efficiency was enhanced with increasing resin contents.

4. Conclusions

A new gelcasting process was successfully used to fabricate fine scale and high green strength piezoelectric pillar arrays through a soft moulding technique using epoxy resin and hardener as gelling system. Relatively low viscous PZT suspensions with solids loading as high as 45 vol.% were electrosterically stabilized based on a synergetic effect between the adsorbed resin molecules having cationic features and an anionic dispersant, Dispex A 40. Pillars with lateral features lower than 10 μm and aspect ratios higher than 10:1 could be easily fabricated using soft reusable PDMS moulds. The flexural strength of the consolidated green bodies increased with increasing added amount of resin in the range of 10–20 wt.% relative to the amount of liquid, achieving a value of 35 MPa for 20 wt.% of added epoxy resin. The sintered PZT ceramics consolidated by this technique show relatively dense and homogeneous microstructures, making the new gelcasting process an attractive choice for fabricating high frequency transducers. The near net shaping capabilities of this new gelcasting process enables elimination of expensive micromachining, therefore decreasing the production costs of the ceramic components. These features represent a huge step

forward in the challenging fabrication of micron or submicron components.

Acknowledgments

S.M. Olhero wishes to thank to Foundation for Science and Technology of Portugal for the financial support under the grant SFRH/BPD/27013/2006. The authors would also like to thank CICECO for the work at the University of Aveiro and FCT for the financial support under the project PTDC/CTM/099489/2008. The support of EPSRC for the work at the University of Birmingham (and the associated design of the moulded structures by Drs. C. Démoré and S. Cochran at the University of Dundee) is also gratefully acknowledged. The authors would also like to thank C. Meggs at the University of Birmingham for his input into the work.

References

1. Lejeune M, Chartier T, Dossou-Yovo C, Noguera R. Ink-jet printing of micro-pillar arrays. *J Eur Ceram Soc* 2009;**29**:905–11.
2. Brown J, Chérin E, Yin J, Foster F. Fabrication and performance of a high-frequency geometrically focussed composite transducer with triangular pillar geometry. *IEEE Ultrason Symp* 2007:80–3.
3. Pazol B, Bowen L, Gentilman R, Pham H, Serwatka W. Ultrafine scale piezoelectric composite materials for high frequency ultrasonic imaging arrays. *IEEE Ultrason Symp* 1995:1263–8.
4. Farlow R, Galbraith W, Knowles M, Hayward G. Micromachining of a piezocomposite transducer using a copper vapor laser. *IEEE Trans Ultrason Ferroelec Freq Control* 2001;**48**:639–40.
5. Ruibin L, Harasiewicz K, Foster F. Interdigital pair bonding for high frequency (20–50 MHz) ultrasonic composite transducers. *IEEE Trans Ultrason Ferroelec Freq Control* 2001;**48**:299–306.
6. Abrar A, Zhang D, Su B, Button TW, Kirk KJ, Cochran S. 1–3 connectivity piezoelectric ceramic–polymer composite transducers made with viscous polymer processing for high frequency ultrasound. *Ultrasonics* 2004;**42**:479–84.
7. Omatete O, Janney M, Strelow R. Gelcasting – a new ceramic forming process. *Ceram Bull* 1991;**70**:1641–9.
8. Young C, Omatete O, Janney M, Menchhofer P. Gelcasting of alumina. *J Am Ceram Soc* 1991;**74**:612–8.
9. Guo D, Cai K, Li L, Nana C, Gui Z. Gelcasting of PZT. *Ceram Int* 2003;**29**:403–6.
10. Guo D, Cai K, Li L, Gui Z. Application of gelcasting to the fabrication of piezoelectric ceramic parts. *J Eur Ceram Soc* 2003;**23**:1131–7.
11. Potoczek M, Zawadzak E. Initiator effect on the gelcasting properties of alumina in a system involving low-toxic monomers. *Ceram Int* 2004;**30**:793–9.
12. Olhero S, Tarì G, Coimbra M, Ferreira JMF. Synergy of polysaccharide mixtures in gelcasting of alumina. *J Eur Ceram Soc* 2000;**20**:423–9.
13. Olhero S, Tarì G, Ferreira JMF. Feedstock formulations for direct consolidation of porcelains with polysaccharides. *J Am Ceram Soc* 2001;**84**(4):719–25.
14. Ganesh I, Jana D, Shaik S, Thiyagarajan N. An aqueous gelcasting process for sintered silicon carbide ceramics. *J Am Ceram Soc* 2006;**89**:3056–64.
15. Roy S, Chandra Rao B, Subrahmanyam J. Water based gelcasting of lead zirconate titanate and evaluation of mechanical properties of the gel cast samples. *Scripta Mater* 2007;**57**:817–20.
16. Sung Soo-HA. Effect of atmosphere type on gelcasting behaviour of Al_2O_3 and evaluation of green strength. *Ceram Int* 2000;**26**:251–4.
17. Ganesh I, Olhero S, Torres P, Alves F, Ferreira J. Hydrolysis induced aqueous gelcasting for near-net shape forming of ZTA ceramic composites. *J Eur Ceram Soc* 2009;**29**:1393–401.
18. Mao X, Shimai S, Dong M, Wang S. Investigation of new epoxy resins for the gel casting of ceramics. *J Am Ceram Soc* 2008;**91**:1354–6.
19. Mao X, Shimai S, Wang S. Gelcasting of alumina foams consolidated by epoxy resin. *J Eur Ceram Soc* 2008;**28**:217–22.
20. Mao X, Shimai S, Dong M, Wang S. Gelcasting of alumina using epoxy resin as a gelling agent. *J Am Ceram Soc* 2007;**90**:986–8.
21. Olhero S, Ferreira J. Influence of particle size distribution on rheology and particle packing of silica-based suspensions. *Powder Technol* 2004;**139**:69–75.
22. Napper D. *Polymeric stabilization of colloidal dispersions*. London: Academic Press; 1983.
23. Lewis J. Colloidal processing of ceramics. *J Am Ceram Soc* 2000;**83**:2341–59.
24. Derjaguin B, Landau L. *Acta Physicochim* 1941;**14**:633.
25. Verwey E, Overbeek J. Theory of stability of lyophobic colloids. Amsterdam; 1948.
26. Overbeek J. In: Kruyt HR, editor. *Colloid science*. Amsterdam: Elsevier, Publ. Co; 1974.
27. Khorsand Z, Majid W. Effect of solvent on structure and optical properties of PZT nanoparticles prepared by sol–gel method, in infrared region. *Ceram Int* 2011;**37**:753–8.
28. Raju K, Reddy P. Synthesis and characterization of microwave processed PZT material. *Curr Appl Phys* 2010;**10**:31–5.
29. Richard A, Nyquist, Ronald O, Kagel. Infrared spectra of Inorganic compounds, 3800–45 cm^{-1}. *Handbook of infrared and Raman spectra of inorganic compounds and organic salts*, 4. San Diego: Academic Press; 1997.
30. Silverstein RM, Bassler GC, Morrill TC. *Spectrometric identification of organic compounds*. 4th ed. New York: John Wiley and Sons; 1981.
31. Chen B, Jiang D, Zhang J, Dong M, Lin Q. Gel casting of β-TCP using epoxy resin as a gelling agent. *J Eur Ceram Soc* 2008;**28**:2889–94.